



## New Systematics in Hadron Total Cross Sections\*

Harry J. Lipkin<sup>†</sup>Argonne National Laboratory, Argonne, Illinois 60439

and

Fermi National Accelerator Laboratory, Batavia, Illinois 60510

## ABSTRACT

Experimental data for the quark model expression  $\sigma(\phi p) = \sigma(K^- p) + \sigma(K^+ p) - \sigma(\pi^- p)$  and the peculiar linear combination  $(3/2)\sigma(K^+ p) - (1/3)\sigma(pp)$  are equal and monotonically rising as  $a + b \log s$  over the entire 2—200 GeV/c range. A new third component exhibiting a striking scaling behavior is shown to be present in total cross sections and to explain these and other unexplained effects: 1) The  $\sigma(\pi N) - \sigma(KN)$  difference, 2) the deviation of  $\sigma(\pi N)/\sigma(NN)$  from 2/3, 3) differences in energy behavior of cross sections, particularly the decrease in  $\sigma(pp)$  at low energies, 4) the differences between  $\sigma(K^+ p)$ ,  $\sigma(pp)$  and  $\sigma(\phi p)$  which are all pure Pomeron in two-component duality.

---

<sup>†</sup> On leave from Weizmann Institute of Science, Rehovot, Israel.



Hadron total cross section data over the energy range from a few GeV to 200 GeV are consistent with predictions from quark models, Regge pole models and various symmetry schemes. However, several apparently unrelated discrepancies exist at the 15% level. The purpose of this letter is to point out a systematic behavior in these unexplained effects and to suggest the presence of a new slowly decreasing component which contributes to KN,  $\pi$ N and NN total cross sections in the ratio of 1:2:9/2. Such a "third component" has been predicted by a theoretical model<sup>1</sup> which agrees with experiment to the level of a few percent. Since the dynamical foundations of this model are not clear, we discuss regularities in the data from a model-independent point of view.

The regularities are most easily seen by examining "reduced total cross sections" for a hadron H on a proton defined by the relations

$$\sigma_R(Hp) \equiv \sigma_{\text{tot}}(Hp) - 1.75(N_{\bar{H}}^H + 2N_p^H)(P_{\text{LAB}}/20)^{-1/2} \quad (1)$$

$$\sigma_{\text{RP}}(Hp) \equiv \sigma_R(Hp) - (N_q^H)[13.5 + 1.25 \log(P_{\text{LAB}}/20)]/2 \quad (2)$$

where all cross sections are in millibarns,  $N_i^H$  is the number of quarks of type i in the incident hadron H and  $N_q^H$  is the total number of quarks and antiquarks in hadron H. Equations (1) and (2) describe the components of  $\sigma_{\text{tot}}(Hp)$  which remain after the dominant Regge and pomeron contributions are removed by simple rules discussed below. The experimental data<sup>2</sup> presented in Table I show the surprising result that  $\sigma_{\text{RP}}$  defined by Eq. (2)

scales in the ratio 1:2:9/2 for KN,  $\pi$ N and NN total cross sections over the entire range from 2 to 200 GeV/c.

The observed hadron-nucleon total cross sections can therefore be described to a few percent as the sum of three components. Two of these correspond to the subtracted terms in Eq. (1) and (2). The third scales in the peculiar 1:2:9/2 ratio and has the magnitude and energy dependence given in Table I. This third component is appreciable even at 200 GeV where it contributes 3.5, 7 and 15 mb to the KN,  $\pi$ N and NN cross sections.

The physical implications of this empirical three-component description can be clarified by a detailed analysis of the experimental data. These are plotted in Fig. 1 with the baryon-nucleon cross sections multiplied by 2/3 to exhibit quantities predicted to be equal by the quark model. Also plotted are the linear combinations

$$\sigma(\phi p) \equiv \sigma_{\text{tot}}(K^+ p) + \sigma_{\text{tot}}(K^- p) - \sigma_{\text{tot}}(\pi^- p) \quad (3a)$$

and

$$\sigma(\text{Pom}) \equiv \frac{3}{2}\sigma_{\text{tot}}(K^+ p) - \frac{1}{3}\sigma_{\text{tot}}(pp). \quad (3b)$$

The expression (3a) for  $\sigma(\phi p)$  is obtained from the quark model and has been used successfully to describe  $\phi$  photoproduction. The expression (3b) describes the "pure pomeron" contribution according to the model of Ref. 1. All the cross sections in Fig. 1 are seen to be equal at the 20% level at 200 GeV/c. But more precise analysis shows several unexplained and apparently unrelated effects.

1. The  $\pi$ N-KN Difference. The difference  $\sigma_{\text{tot}}(\pi^- p) - \sigma_{\text{tot}}(K^- p)$  is 5 mb at 2 GeV/c and decreases slowly to about 3.5 mb at 200 GeV/c. This slowly decreasing strangeness-dependent contribution to the total cross section is larger than the contributions from the leading Regge exchanges at NAL energies and is not explained by any dynamical or symmetry theory. Attributing the difference to SU(3) symmetry breaking or to a difference between strange and nonstrange quarks<sup>3</sup> simply introduces one new free parameter with unknown energy dependence to fit one new effect in the data.

2. The Deviation from the Levin-Frankfurt 3/2 Rule. The cross sections  $(2/3)\sigma_{\text{tot}}(pp)$  and  $(2/3)\sigma_{\text{tot}}(\bar{p}p)$  are not equal to  $\sigma(\pi p)$  and  $\sigma(Kp)$  as predicted by the quark model<sup>4</sup> but are consistently higher by about 20%. This effect cannot be explained in the additive quark model and indicates the presence of a non-additive contribution. Although a 20% discrepancy in predictions from the additive quark model is not surprising, this discrepancy has not been explained by a more precise description nor related to other phenomena such as the  $\pi$ N-KN difference.

3. The Pomeron Contribution. Duality<sup>5</sup> and exchange degeneracy suggest that the "pure" pomeron contribution should be seen in  $\sigma_{\text{tot}}(K^+ p)$  and  $\sigma_{\text{tot}}(pp)$  which are exotic and have no contributions from the leading Regge exchanges. The pure pomeron should also appear in  $\sigma_{\text{tot}}(\phi p)$  since the  $\phi$  consists only of strange quarks and is not coupled to the leading Regge trajectories. However, the experimental data for

$\sigma_{\text{tot}}(K^+ p)$ ,  $\sigma_{\text{tot}}(pp)$  and the quark model expression (3a) for  $\sigma(\phi p)$  behave very differently as a function of energy between 2 and 200 GeV/c. If one is the pure pomeron the other two are not, an additional contribution must be present to explain the difference between these cross sections and the pure pomeron.

4. Different Behaviors of Rising Cross Sections. Rising total cross sections were noticed in the Serpukhov data<sup>2</sup> from 20—60 GeV/c and confirmed at higher energies. However, each curve in Fig. 1 shows a different energy behavior. Striking features not previously noted are the monotonic rising behavior and the approximate equality of the particular linear combinations of cross sections (3a) and (3b) over the entire energy range from 2 to 200 GeV/c. The equality is not predicted by any theoretical description except for the model of Ref. 1.

We now show that all these apparently unrelated effects seem to have a single common explanation. Our approach is to subtract from the experimental total cross section data the well-understood contributions given by established rules of two-component duality or exchange degeneracy. The remaining portions of the total cross section data are then examined and found to exhibit remarkably simple features.

Equation (1) is obtained from a simple recipe for removing the contributions of the leading exchange-degenerate Regge trajectories  $\rho$ ,  $\omega$ ,  $f$  and  $A_2$ . These are known to vary with energy approximately as  $s^{-1/2}$  and to be proportional to a "quark counting factor" given by strong exchange

degeneracy or duality diagrams<sup>5</sup> to be the number of possible annihilations between an antiquark in hadron H and a quark of the same kind in the target proton. The coefficient  $1.75 \times (20)^{1/2}$  was determined empirically by fitting the data. The experimental values of  $\sigma_R$  are shown in Fig. 2. That the empirical expression (1) indeed removes the major portion of the leading Regge exchange is indicated by the collapse of the particle-antiparticle differences to give three curves independent of charge for  $(2/3)\sigma(NN)$ ,  $\sigma(\pi N)$  and  $\sigma(KN)$  above 10 GeV/c.

Two-component duality describes the quantities plotted in Fig. 2 as the pomeron contribution to the total cross section, since their Regge contributions are removed. They are all expected to be equal in the Levin-Frankfurt approximation. The data show a striking new regularity in the departure from equality, an approximately equal spacing all the way from 2 to 200 GeV/c not predicted by any theory except the model of Ref. 1. The pion-kaon difference appears to be related to the discrepancy from the Levin-Frankfurt  $3/2$  ratio between baryon-baryon and meson-baryon cross sections, although the former is usually attributed to SU(3) symmetry breaking and the latter completely unrelated to SU(3).

Equation (2) is obtained from a simple recipe for removing the "pomeron" contribution, assumed to satisfy the Levin-Frankfurt ratio of  $1:1:3/2$  for KN,  $\pi N$  and NN cross sections. Since the linear combinations (3a) and (3b) show a very simple energy behavior, consistent with the parametrization  $a + b \log s$  over the entire range from 2 to 200 GeV/c,

we assume that these represent the pomeron.<sup>6</sup> The parameters in Eq. (2) were determined by a straight line fit to the data. Experimental values of  $\sigma_{RP}$  are shown in Fig. 3. The three curves representing  $\sigma_{RP}(\text{KN})$ ,  $\sigma_{RP}(\pi\text{N})$  and  $\sigma_{RP}(\text{NN})$  are seen to scale with the same energy dependence and a ratio 1:2:3. This is emphasized by plots of the same data in Fig. 4 as a universal curve when  $\sigma_{RP}(\text{KN})$ ,  $\sigma_{RP}(\pi\text{N})$  and  $\sigma_{RP}(\text{NN})$  are multiplied by scaling factors  $3:\frac{3}{2}:\frac{2}{3}$ .

The spread in the curves at low energies in Figs. 2—4 indicate that the prescription (1) for removing the Regge exchange component has not completely removed the charge dependence of the cross sections at low energies. Some additional contribution is present such as a lower trajectory or a cut. Without attempting to explore the nature of this contribution we note that the scaling of  $\pi\text{N}$ ,  $\text{KN}$  and  $\text{NN}$  cross sections in Fig. 4 is even more marked when the lowest charge states  $\sigma(\text{pp})$ ,  $\sigma(\pi^- \text{p})$  and  $\sigma(\text{K}^+ \text{p})$  are chosen. These are given in the first three columns in Table I. There is no obvious reason why these particular charge states should scale all the way down to 2 Gev/c. Although the  $\text{K}^+ \text{p}$  and  $\text{pp}$  channels are exotic the  $\pi^- \text{p}$  channel is not. Any deeper significance in the choice of these particular charge states must result from the behavior of the non-leading component responsible for charge differences at low energies.

Table I and Figs. 3—4 present striking evidence for a third component in hadron total cross sections which decreases slowly with

energy and satisfies the ratio  $1:2:9/2$ . A search for a dynamical model which can give rise to such a component is therefore of interest. The data presented here do not indicate whether this third component should decrease to zero at very high energies or approach a constant. Using higher energy ISR data for  $\sigma(pp)$  in Eq. (2) gives inconclusive results, because slight changes in the parameters of Eq. (2) give significant differences at higher energies while having a negligible effect on the plots of Fig. 3. Without some theoretical basis for choosing the form and parametrization of Eq. (2), it is impossible to extrapolate these results to higher energies.

Another use of this apparent regularity is to study the two better-known components by using the  $1:2:9/2$  ratio to eliminate the mysterious third component. The linear combination (3b) is chosen in this way and represents some "true pomeron" part of  $\sigma(K^+p)$  and  $\sigma(pp)$ . This linear combination might be useful in testing models for rising cross sections, since it rises consistently from 2 to 200 GeV/c in contrast to  $\sigma(K^+p)$  and  $\sigma(pp)$  which show very different behavior at lower energies.

Linear combinations which eliminate the pomeron and the third component should contain contributions from only the exchange-degenerate Regge trajectories. These have been shown<sup>1</sup> to decrease like  $s^{-1/2}$  as expected and to enable the separation of the pomeron and  $f$  contributions in isoscalar even signature amplitudes. Such linear combinations have the form<sup>1</sup>

$$A_{\text{Reg}} = A(\pi p) - \frac{1}{2}A(Kp) - \frac{1}{3}A(pp) \quad (4)$$

where the amplitudes  $A(\pi p)$ ,  $A(Kp)$  and  $A(pp)$  denote any charge state of the system or any linear combination of amplitudes for different charge states with coefficients whose sum is unity.

The relation (4) might also be applied to amplitudes obtained from differential cross sections and be useful to separate out a Regge-exchange term, particularly in the even signature isoscalar exchange which contains the pomeron. However, linear combinations of amplitudes are not easily available from data on differential cross sections which are sums of squares of flip and non-flip amplitudes. For a rough test of this approach we assume that experimental data at low values of  $t$  are dominated by the imaginary part of the non-flip amplitude. This amplitude is then approximately given by the square root of the differential cross section. Figure 5 shows plots from data<sup>7</sup> at 6 GeV/c of several linear combinations of square roots of differential cross sections having the form (4) and normalized to be equal if the Regge component is given by duality diagrams.

$$\Delta(Kp) \equiv A(K^- p) - A(K^+ p) \quad (5a)$$

$$\omega_1 \equiv \frac{1}{3}[A(\bar{p}p) - A(pp)] \quad (5b)$$

$$\omega_2 \equiv \frac{1}{3}[A(\bar{p}p) - A(pp) + A(\pi^- p) - A(\pi^+ p)] \quad (5c)$$

$$f_1 \equiv A(\pi^- p) - \frac{1}{2}A(K^+ p) - \frac{1}{3}A(pp) \quad (6a)$$

$$f_2 \equiv 2A(\pi^+ p) - A(K^+ p) - \frac{2}{3}A(pp) \quad (6b)$$

$$f_3 \equiv \frac{2}{5}A(\bar{p}p) + \frac{3}{5}A(K^- p) - \frac{6}{5}A(\pi^+ p) \quad (6c)$$

The linear combinations (5) of particle-antiparticle cross section differences are known to be described to a good approximation by the exchange of odd-signature Regge trajectories and to satisfy  $\rho$  and  $\omega$  universality relations. Figure 5 shows that  $\Delta(Kp)$ ,  $\omega_1$  and  $\omega_2$  have the form of a typical Regge exchange contribution and exhibit a crossover in the neighborhood of  $t = 0.2$ . The equality of these three curves in Fig. 5 in agreement with universality predictions suggests that the use of square roots of cross sections as amplitudes is a good approximation.

The three linear combinations (6) are new and not predicted by any previous theories to behave in any simple way. The expressions (6a) and (6b) use the recipe (4) to remove the pomeron component from the pion-nucleon amplitude and leave only the  $f$  and  $\rho$  exchange components. The expressions  $f_1$ ,  $f_2$  and  $f_3$  are seen to behave qualitatively as expected with a peak at  $t = 0$  and a crossover at a value of  $t$  between 0 and 0.5. Quantitatively, there are significant deviations from the prediction that  $f_1 = f_2 = f_3 = \Delta(Kp)$  in the limit of universal couplings and strong exchange degeneracy. These discrepancies may indicate that the recipe (4) is not as good at finite values of  $t$  as at  $t = 0$ , that the spin-flip and real-part components of the amplitudes are not negligible in these linear combinations while they tend to cancel in the total cross section differences, or that 6 GeV/c is still too low an energy for quantitative agreement. However, the qualitative agreement suggests that the recipe (4) indeed removes the main portion of the pomeron from the amplitudes considered. The pomeron itself is positive definite and should not exhibit

any crossover. It would be a remarkable coincidence for an arbitrary linear combination of  $\pi N$ ,  $KN$  and  $NN$  cross sections to show this qualitative behavior. Further investigation of the validity of the prescription (4) would be of interest both at higher energies and in cases where the real and imaginary or slip and non-flip components of the amplitude can be separated experimentally.

It is a pleasure to thank Dr. Stanley Cohen and members of the Argonne Speakeasy group for instruction, assistance and encouragement in the use of Speakeasy for rapid computation and plotting of functions of the total cross section data. Figures 1—5 are direct copies of Speakeasy plots on the Tektronix oscilloscope.

## References and Footnotes

\*Work performed under the auspices of the U.S. Atomic Energy Commission.

<sup>1</sup>H. J. Lipkin, A "Three-Component" Model for Hadron Total Cross Sections, Weizmann Institute preprint WIS-74/17-Ph, to be published in Nuclear Physics.

<sup>2</sup>E. Flaminio, J. D. Hansen, D. R. O. Morrison, N. Tovey, Compilation of Cross Sections. I. Proton Induced Reactions. II. Antiproton Induced Reactions, CERN/HERA 70-2 and 70-3; E. Bracci, J. P. Droulez, E. Flaminio, J. D. Hansen and D. R. O. Morrison, Compilation of Cross Sections. I.  $\pi^-$  and  $\pi^+$  Induced Reactions. II.  $K^-$  and  $K^+$  Induced Reactions, CERN/HERA 72-1 and 72-3; J. B. Allaby, Yu. B. Bushnin, Yu. P. Gorin et al., Yad. Fiz. 12 (1970) 538; Phys. Letters 30B (1969) 500; Yu. P. Gorin, S. P. Denisov, S. V. Donskov et al., Yad. Fiz. 14 (1971); Phys. Letters 36B (1971) 415; S. P. Denisov, S. V. Donskov, Yu. P. Gorin et al., Nucl. Phys. B65 (1973) 1; A. S. Carroll et al., Total Cross Sections of P and  $\bar{P}$  on Protons and Deuterons between 50 and 200 GeV/c, NAL-Pub-74/75-EXP (July 1974); A. S. Carroll et al., Total Cross Sections of  $\pi^\pm$  and  $K^\pm$  on Protons and Deuterons between 50 and 200 GeV/c, NAL-Pub-74/76-EXP (July 1974).

<sup>3</sup>H. J. Lipkin, Phys. Rev. Letters 16 (1966), 1015; H. J. Lipkin, Z. Phys. 202 (1967), 414.

<sup>4</sup>E. M. Levin and L. L. Frankfurt, ZhETF Pisma 2 (1965); JETP Letters (Sov. Phys.) 2 (1965), 65; H. J. Lipkin and F. Scheck, Phys. Rev. Letters 16 (1966), 71.

<sup>5</sup>M. Kugler, Acta Phys. Austriaca Suppl. VII (1970), 443 and references therein; H. J. Lipkin, Nucl. Phys. B9 (1969), 349; H. Harrari, Phys. Rev. Letters 22 (1969), 562; J. L. Rosner, Phys. Rev. Letters 22 (1969), 689.

<sup>6</sup>The term Pomeron is used here to denote that part of the total cross section which satisfies the Levin-Frankfurt ratio 1:1:3/2. It is not necessarily the entire diffractive component and may be only a piece of what is called the Pomeron in other treatments. The "third component" discussed in this paper could well be an additional component of the Pomeron which satisfies the ratio 1:2:9/2 instead of the Levin-Frankfurt ratio for some unknown dynamical reason.

<sup>7</sup>I. Ambats et al., Phys. Rev. D 9, 1179 (1974).

## Figure Captions

- Fig. 1. Experimental total cross section data and the linear combinations (3).
- Fig. 2. Reduced total cross sections—Regge component removed by Eq. (1).
- Fig. 3. Reduced total cross sections—two components removed by Eq. (2).
- Fig. 4. Scaled reduced total cross sections given by Eq. (2). Quantities plotted are  $(2/3)\sigma_{RP}(NN)$ ,  $(3/2)\sigma_{RP}(\pi N)$  and  $3\sigma_{RP}(KN)$ .
- Fig. 5. Plots of amplitude differences (5) and (6) at 6 GeV/c.

TABLE I. Experimental values of  $\sigma_{RP}$  suitably scaled.

| P     | $\sigma_{RP}(K^+p)$ | $\frac{1}{2}\sigma_{RP}(\pi^-p)$ | $\frac{2}{9}\sigma_{RP}(pp)$ | $\sigma_{RP}(K^-p)$ | $\frac{1}{2}\sigma_{RP}(\pi^+p)$ | $\frac{2}{9}\sigma_{RP}(\bar{p}p)$ |
|-------|---------------------|----------------------------------|------------------------------|---------------------|----------------------------------|------------------------------------|
| GeV/c | mb                  | mb                               | mb                           | mb                  | mb                               | mb                                 |
| 2     | 7.0                 | 7.1                              | 6.9                          | 8.4                 | 6.5                              | 10                                 |
| 3     | 6.1                 | 6.1                              | 6.2                          | 7.2                 | 6.8                              | 8.3                                |
| 6     | 5.0                 | 5.1                              | 5                            | 5.6                 | 5.5                              | 5.6                                |
| 8     | 4.9                 | 4.8                              | 4.8                          | 5.7                 | 5.2                              | 5.3                                |
| 10    | 4.7                 | 4.6                              | 4.7                          | 4.9                 | 4.9                              |                                    |
| 12    | 4.4                 | 4.5                              | 4.5                          | 4.2                 | 4.7                              | 4.7                                |
| 14    | 4.3                 | 4.4                              | 4.3                          | 4.3                 | 4.5                              | 4.6                                |
| 16    | 3.8                 | 4.3                              | 4.2                          | 4.2                 | 4.4                              | 4.4                                |
| 18    | 3.7                 | 4.2                              | 4.1                          | 3.9                 | 4.3                              | 4.7                                |
| 15    | 4.2                 | 4.3                              | 4.4                          | 4.4                 | 4.5                              | 4.7                                |
| 20    | 3.9                 | 4.1                              | 4.2                          | 4.0                 | 4.1                              | 4.3                                |
| 25    | 3.9                 | 3.9                              | 4.0                          | 3.8                 | 4.0                              | 4.1                                |
| 30    | 3.7                 | 3.8                              | 3.9                          | 4.0                 | 3.9                              | 3.9                                |
| 35    | 3.6                 | 3.8                              | 3.8                          | 3.6                 | 3.8                              | 3.9                                |
| 40    | 3.7                 | 3.7                              | 3.8                          | 3.7                 | 3.7                              | 3.8                                |
| 45    | 3.4                 | 3.7                              | 3.7                          | 3.7                 | 3.7                              | 3.7                                |
| 50    | 3.7                 | 3.7                              | 3.7                          | 3.6                 | 3.7                              | 3.5                                |
| 55    | 3.4                 | 3.8                              | 3.6                          | 3.6                 | 3.7                              |                                    |
| 50    | 3.4                 | 3.6                              | 3.6                          | 3.4                 | 3.7                              | 3.6                                |
| 100   | 3.3                 | 3.4                              | 3.4                          | 3.3                 | 3.5                              | 3.3                                |
| 150   | 3.3                 | 3.4                              | 3.2                          | 3.3                 | 3.4                              | 3.2                                |
| 200   | 3.5                 | 3.4                              | 3.2                          | 3.4                 | 3.4                              | 3.2                                |

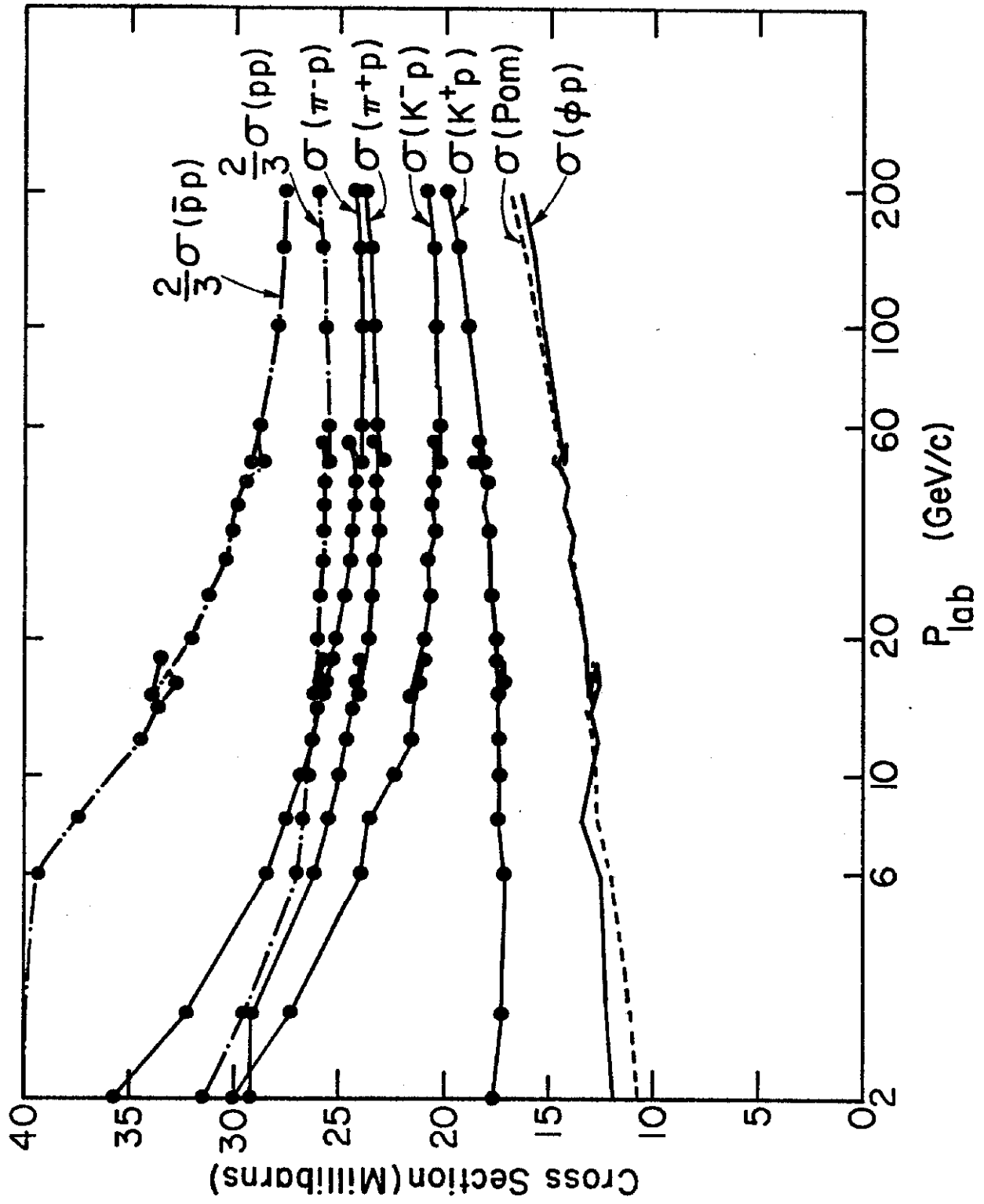


Fig. 1

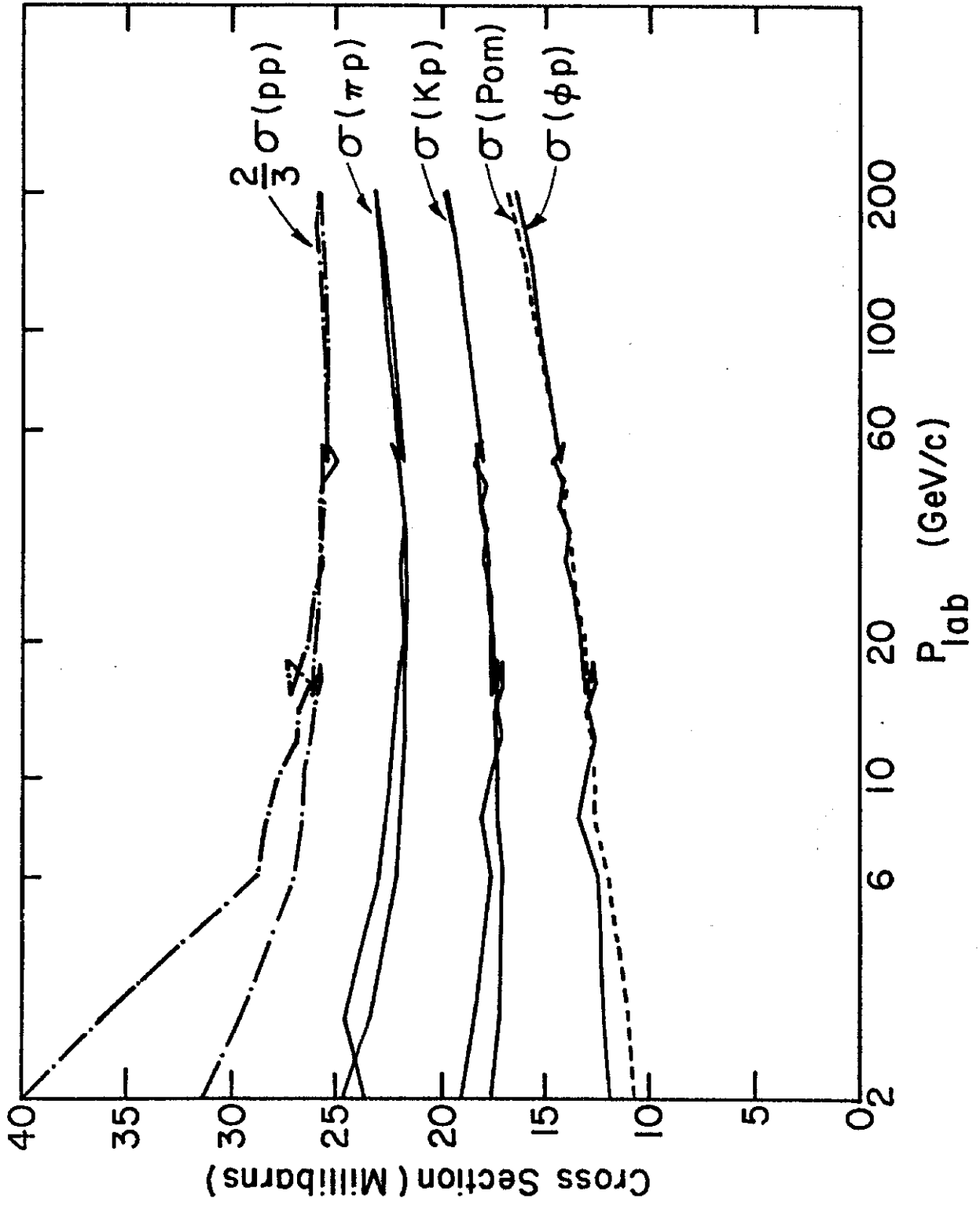


Fig. 2

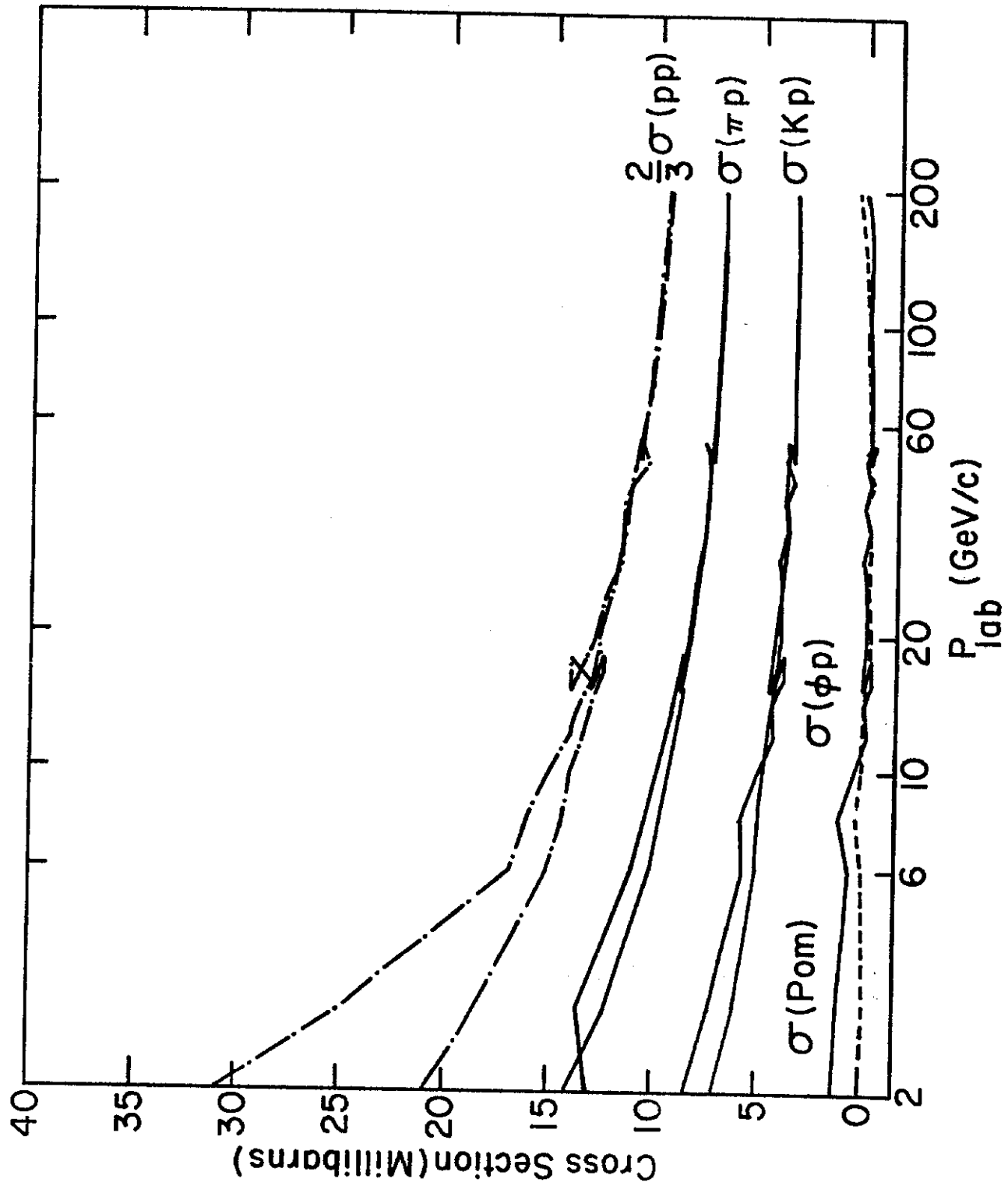


Fig. 3

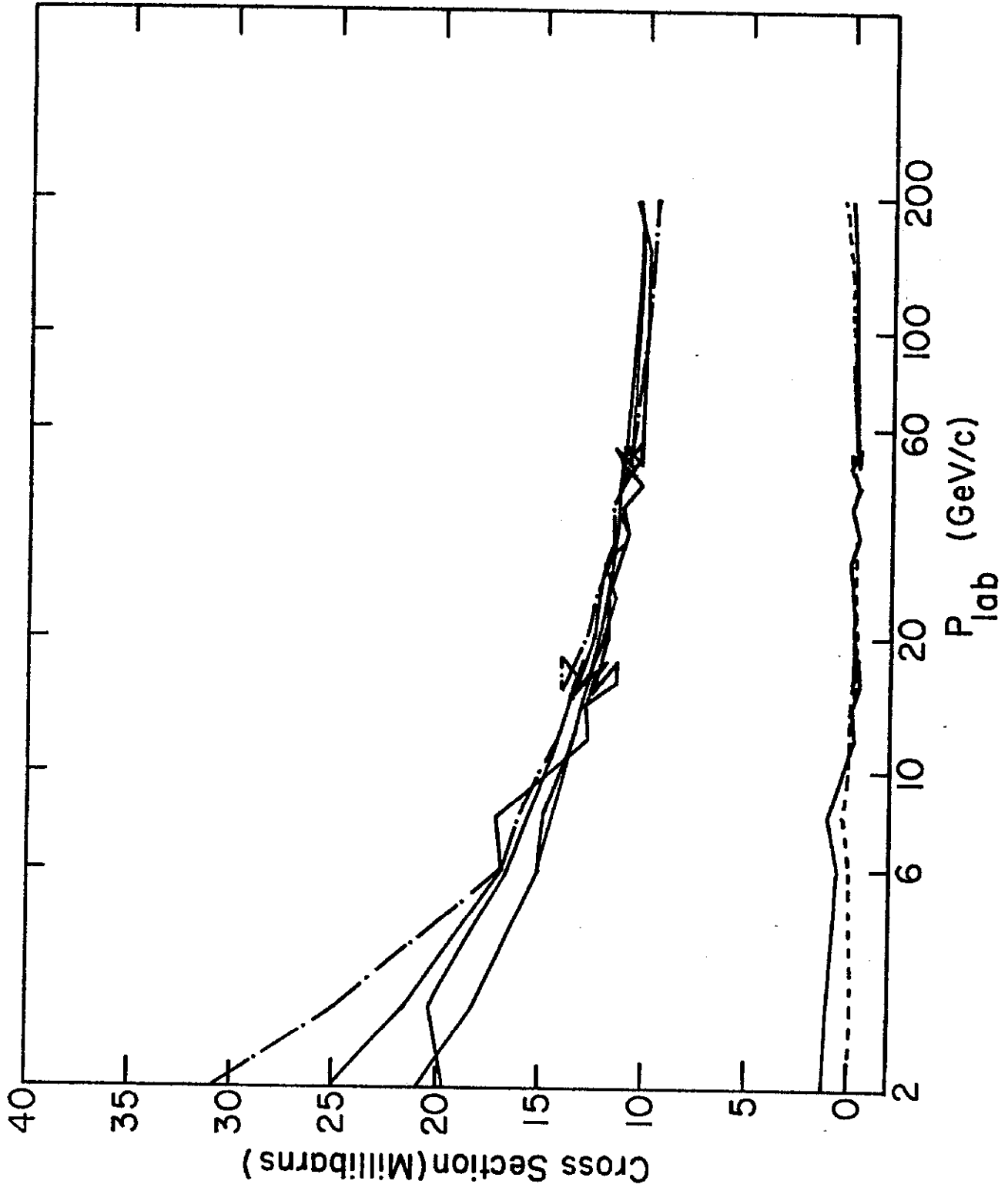


Fig. 4

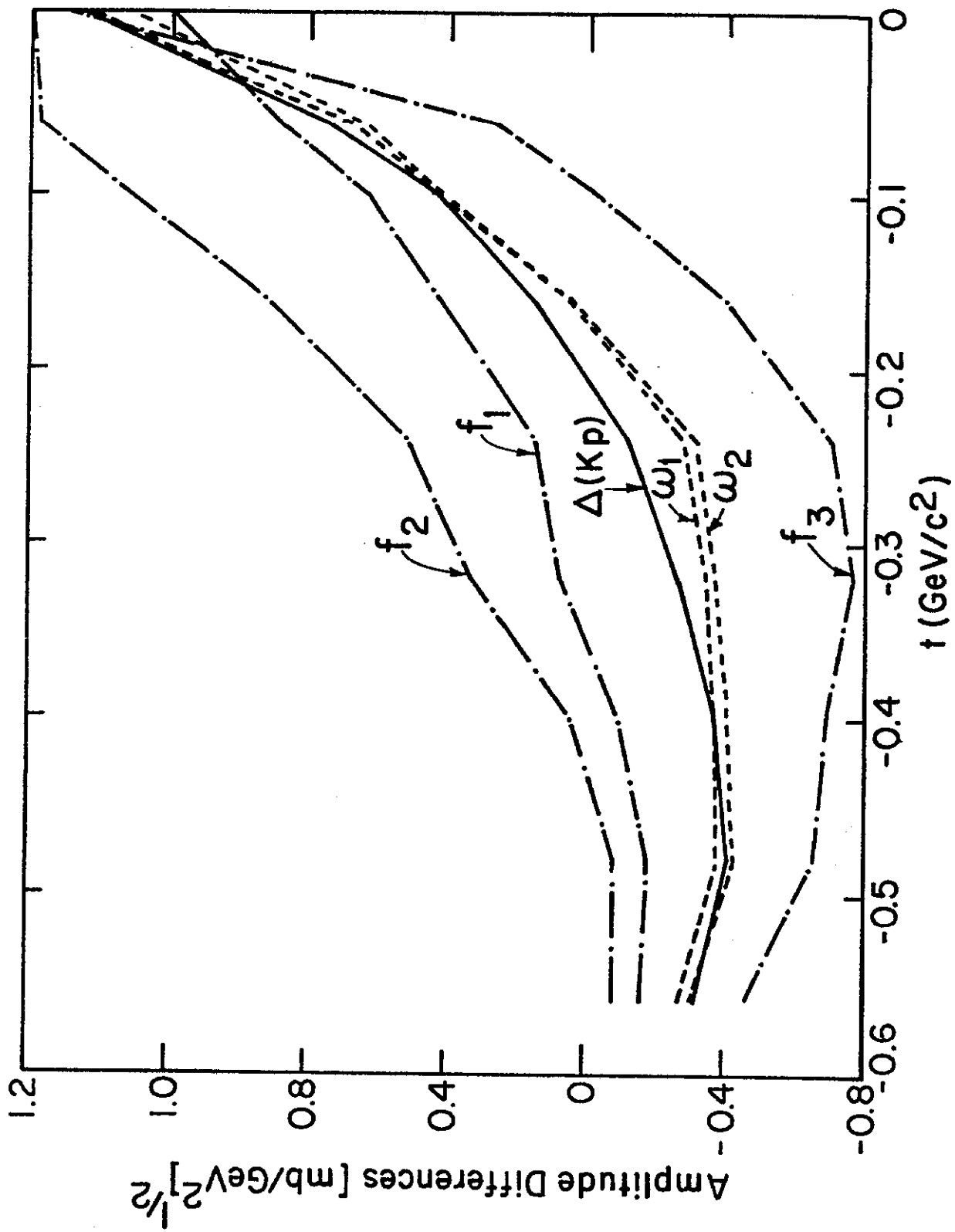


Fig. 5